Retrospective Cost Adaptive Control for Helicopter Vibration Reduction

Ashwani K. Padthe
Postdoctoral Researcher
akpadthe@umich.edu

Peretz P. Friedmann
François-Xavier Bagnoud
Professor of Aerospace Engineering
peretzf@umich.edu

Dennis S. Bernstein
Professor
dsbaero@umich.edu

Department of Aerospace Engineering
University of Michigan, Ann Arbor, Michigan

Abstract

A retrospective cost adaptive controller (RCAC) is examined for helicopter vibration reduction using active trailing-edge flaps. Vibration reduction performance of the RCAC controller is compared to that of the adaptive Higher harmonic controller (HHC) on a hingeless rotor configuration resembling the MBB BO-105 equipped with a single 20%c trailing-edge flap on each of the blades. The comparison is performed at both a low-speed descending flight condition and a high-speed cruise condition. A linear approximate model of the dynamics between the vibratory loads and control surface deflections is used as the system information in the controllers. Robustness of the two controllers to errors in the approximate model is analyzed and compared. Robustness of the controllers to variations in the helicopter weight coefficient is also compared. The results show that the RCAC is as effective as the HHC and due to its adaptive nature, the RCAC has considerable potential for more complicated rotorcraft missions involving maneuvering flight.

Nomenclature

b	Rotor blade semi-chord $= \frac{c_b}{2}$
c_b	Rotor blade chord
C_{df}	Fuselage drag coefficient
C_W	Helicopter weight coefficient
D_0, D_1	Generalized flap motions
e	Blade root offset from center of rotation
f	Equivalent flat plate area of the fuselage
F_{HX4}, F_{HY4}, F_{HZ4}	4/rev components of hub shear
F_{HZ4c}, F_{HZ4s}	cosine and sine components of F_{HZ4}
G_{zu}	Transfer function relating the input and performance
$\mathcal{H}_i$	Markov parameters of G_{zu}
J	Quadratic cost function
J_z	Retrospective cost function
k	Reduced frequency $= 2\pi\nu b/U$
L_b	Blade length
M	Mach number
M_b	Blade mass
M_{HX4}, M_{HY4}, M_{HZ4}	4/rev components of hub moment
N_b	Number of rotor blades
$P(k)$	Error covariance matrix
$\mathbf{Q}$	Weighting on the output vector
R	Rotor blade radius
$\mathbf{R}$	Weighting on the control input
$\mathbf{T}$	Sensitivity matrix relating control input to the plant output
$\hat{\mathbf{T}}_{\mathrm{LS}}$	Least squares estimate of $\mathbf{T}$
t	Time
$\bar{t}$	Reduced time $= \frac{1}{b}\int_0^t U(\tau)d\tau$
$U(t)$	Freestream velocity, time-dependent

Presented at the American Helicopter Society 69th Annual Forum, Phoenix, Arizona, May 21-23, 2012.

$\mathbf{u}$	control input vector
$\mathbf{w}$	Disturbance
X_A	Offset between the aerodynamic center and the elastic axis
X_{Ib}	Offset of the blade cross-sectional center of mass from the elastic axis
X_{FA}, Z_{FA}	Longitudinal and vertical offsets between rotor hub and helicopter aerodynamic center
X_{FC}, Z_{FC}	Longitudinal and vertical offsets between rotor hub and helicopter center of gravity
$\mathbf{z}$	Plant output vector or performance vector
$\hat{z}$	Retrospective performance
α_{11}, α_{12} α_{21}, α_{22}	Error terms in sensitivity matrix $\mathbf{T}$
α_R	Rotor shaft angle
β_p	Blade precone angle
γ	Lock number
δ_f	Flap or microflap deflection
δ_{Nc}, δ_{Ns}	N/rev cosine and sine amplitudes of δ_f
δ_{limit}	saturation limit on the control surface deflection
δ_{opt}	optimal control surface deflection
μ	Advance ratio
θ_{tw}	Blade pretwist distribution
σ	Rotor solidity
$\omega_F, \omega_L, \omega_T$	Blade flap, lag and torsional natural frequencies
Ω	Rotor angular speed
ψ	Azimuth angle

Introduction and Background

Vibration reduction in rotorcraft using active control has been a major area of research during the last three decades. In addition to causing crew and passenger discomfort, vibrations reduce the airframe and component fatigue life and limit rotorcraft performance resulting in high maintenance costs. During the last three decades, several active control approaches, such as the higher harmonic control (HHC) [1, 2], individual blade control (IBC) [3, 4], the actively controlled trailing-edge flaps (ACF) [5–7], the active twist rotor (ATR) [8], and the microflaps [9] have been explored for rotorcraft vibration reduction. The higher harmonic control (HHC) algorithm has been used in closed-loop vibration reduction studies using the trailing-edge flaps [10] and more recently microflaps [9]. A detailed description of the algorithm, including robustness and stability analysis, can be found in Ref. 10. The HHC algorithm is based on a linear approximation of the dynamics between the vibratory loads and control surface deflections for a steady state. Such an approximation is valid only when the flight condition does not change significantly. Modern rotorcraft are designed for missions involving significant variations in the airframe vibration characteristics due to changes in the aircraft gross weight as a result of fuel consumption or cargo deployment. Furthermore, modern rotorcraft designs are moving towards variable rotor speed configurations for improved performance. The HHC controller lacks robustness to rotor RPM variations since it is based on prior knowledge of the vibration harmonics that need to be reduced. The cost of modeling a helicopter over a wide range of operating conditions can be exorbitant. Therefore, vibration control in advanced rotorcraft systems requires a robust and adaptive controller that can accommodate large variations in the rotorcraft dynamic response.

The primary objective of this paper is to introduce and evaluate such an adaptive controller for helicopter vibration reduction applications. Minimizing the amount of modeling information needed for control is the primary motivation for adaptive control design. However, adaptive control algorithms may involve restrictive assumptions, such as full-state feedback, minimum-phase zeros, and bounds on parameters. To overcome some of these restrictions, a retrospective cost adaptive control (RCAC) algorithm [11–13] was developed at the University of Michigan. The RCAC control algorithm is applicable to both single-input, single-output (SISO) and multi-input, multi-output (MIMO) plants that may be unstable and non-minimum phase with an uncertain disturbance spectrum. The modeling information required by RCAC is limited to a number of Markov parameters. The Markov parameters of a linear time-invariant (LTI) system are its impulse response samples. Any LTI system is completely characterized by its impulse response and hence by the set of all the Markov parameters. In the SISO case, RCAC requires the knowledge of a single nonzero Markov parameter, while in the MIMO case, the number of Markov parameters required depends on the relative number of inputs and

outputs as well as on the rank or numerical conditioning of the Markov parameters. Another distinguishing aspect of RCAC compared to many adaptive control methods is the fact that it is a direct digital control approach. Hence, it bypasses the additional step of controller digitization. In this paper, the performance of the RCAC controller in reducing helicopter vibration reduction is evaluated and compared to the classical HHC controller. A linear approximation of the dynamics between the vibratory loads and the control surface deflections is used as the model information for both controllers. Robustness of the controllers to errors in the linear approximation is also compared. The comprehensive rotorcraft simulation code AVINOR (Active Vibration and Noise Reduction) [14] is used in all the studies presented in this paper. The specific objectives of the proposed paper are:

1. Evaluate the performance of the RCAC controller for reducing vibrations on a representative hingeless rotor configuration, using a comprehensive rotorcraft simulation code.

2. Compare the performance of the RCAC controller to the classical HHC algorithm implemented using a 20%c conventional plain trailing-edge flap.

3. Compare the RCAC and HHC controllers in terms of their robustness to modeling errors at both a low speed flight condition with blade-vortex interaction (BVI) and a high speed flight condition.

4. Compare the robustness of the controllers to variation in the helicopter weight coefficient.

Rotorcraft Aeroelastic Analysis Code

Active control simulations are performed using a comprehensive rotorcraft aeroelastic response code AVINOR which was validated in previous studies [5,14,15]. The principal ingredients of the AVINOR code are concisely summarized next.

Structural dynamic model

The structural dynamic model used in this study consists of a four-bladed hingeless rotor, having fully coupled flap-lag-torsional dynamics for each blade. The structural dynamic model is geometrically nonlinear, due to moderate blade deflections. The structural equations of motion are discretized using the global Galerkin method, based upon the free vibration modes of the rotating blade. The dynamics of the blade are represented by three flap, two lead-lag, and two torsional modes. Free vibration modes of the blade were obtained using the first nine exact non-rotating modes of a uniform cantilevered beam. The code also has the option of modeling the blades using a finite-element method. The effects of control surfaces such as the trailing-edge plain flap on the structural properties of the blade are neglected. Thus, the control surfaces influence the blade behavior only through their effect on the aerodynamic and inertial loads.

Aerodynamic model

The blade/flap sectional aerodynamic loads for attached flow are calculated using a rational function approximation (RFA) based reduced order model constructed from doublet-lattice based aerodynamic data [16]. This model provides unsteady lift, moment, and hinge moment for the plain flap configurations. A more sophisticated CFD based RFA model that can predict drag in addition to lift, moment, and hinge moment due to flaps and microflaps is also available in the code. However, the primary objective of this study is to compare the controllers and therefore the original RFA model is used due to its computational efficiency. The RFA model is linked to a free wake model [5, 15], which produces a spanwise and azimuthally varying inflow distribution. In the separated flow regime aerodynamic loads are calculated using the ONERA dynamic stall model [5].

Coupled aeroelastic response/trim solution

The combined structural and aerodynamic equations are represented by a system of coupled ordinary differential equations with periodic coefficients in state-variable form. The trim is enforced by a propulsive trim procedure where three force equations (longitudinal, lateral, and vertical) and three moment equations (roll, pitch, and yaw) corresponding to a helicopter in free flight are implemented. A simplified tail rotor model, based on uniform inflow and blade element theory, is used. The six trim variables are the rotor shaft angle α_R, the collective pitch θ_0, the cyclic pitch θ_{1s} and θ_{1c}, the tail

rotor constant pitch θ_{0t}, and lateral roll angle ϕ_R. The coupled trim/aeroelastic equations are solved in time using a predictor-corrector ODE solver DDE-ABM, based on the Adams-Bashforth differential system solver.

The Higher Harmonic Control Algorithm

The HHC algorithm has been used extensively for active control of vibration and noise in rotorcraft [5,10]. The algorithm is based on the assumption that the helicopter can be represented by a linear model relating the output of interest $\mathbf{z}$ to the control input $\mathbf{u}$. The measurement of the plant output and update of the control input are performed at specific times $t_k = k\tau$, where τ is the time interval between updates during which the plant output reaches a steady state. In actual implementation of the algorithm, this time interval may be one or more revolutions. A schematic of the HHC architecture implemented on a helicopter is shown in Fig. 1. The disturbance $\mathbf{w}$ represents the helicopter operating condition. The output vector at the k^{th} time step is given by

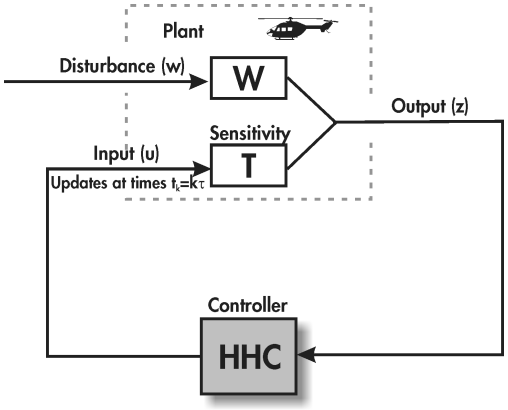

Figure 1: Higher harmonic control architecture

$$\mathbf{z}_k = \mathbf{T}\mathbf{u}_k + \mathbf{W}\mathbf{w} \tag{1}$$

where the sensitivity matrix $\mathbf{T}$ represents a linear approximation of the helicopter response to the control and is given by

$$\mathbf{T} = \frac{\partial \mathbf{z}}{\partial \mathbf{u}}. \tag{2}$$

At the initial condition, $k = 0$,

$$\mathbf{z}_0 = \mathbf{T}\mathbf{u}_0 + \mathbf{W}\mathbf{w}. \tag{3}$$

Subtracting Eq. (3) from Eq. (1) to eliminate the unknown $\mathbf{w}$ yields

$$\mathbf{z}_k = \mathbf{z}_0 + \mathbf{T}(\mathbf{u}_k - \mathbf{u}_0). \tag{4}$$

The controller is based on the minimization of a general quadratic cost function

$$J(\mathbf{z}_k, \mathbf{u}_k) = \mathbf{z}_k^{\mathrm{T}}\mathbf{Q}\mathbf{z}_k + 2\mathbf{z}_k^{\mathrm{T}}\mathbf{S}\mathbf{u}_k + \mathbf{u}_k^{\mathrm{T}}\mathbf{R}\mathbf{u}_k. \tag{5}$$

In most applications, the cross-weighting term in Eq. (5) is neglected thus the cost function reduces to

$$J(\mathbf{z}_k, \mathbf{u}_k) = \mathbf{z}_k^{\mathrm{T}}\mathbf{Q}\mathbf{z}_k + \mathbf{u}_k^{\mathrm{T}}\mathbf{R}\mathbf{u}_k. \tag{6}$$

The optimal control input is determined from the requirement

$$\frac{\partial J(\mathbf{z}_k, \mathbf{u}_k)}{\partial \mathbf{u}_k} = 0, \tag{7}$$

which yields the optimal control law $\mathbf{u}_{k,\mathrm{opt}}$, given by

$$\mathbf{u}_{k,\mathrm{opt}} = -(\mathbf{T}^{\mathrm{T}}\mathbf{Q}\mathbf{T} + \mathbf{R})^{-1}(\mathbf{T}^{\mathrm{T}}\mathbf{Q})(\mathbf{z}_0 - \mathbf{T}\mathbf{u}_0). \tag{8}$$

Combining Eqs. (4), (6) and (8), the minimum cost is

$$J(\mathbf{z}_k, \mathbf{u}_{k,\mathrm{opt}}) \tag{9}$$

$$= (\mathbf{z}_0 - \mathbf{T}\mathbf{u}_0)^{\mathrm{T}} \left[\mathbf{Q} - (\mathbf{Q}\mathbf{T})\mathbf{D}^{-1}(\mathbf{T}^{\mathrm{T}}\mathbf{Q})\right](\mathbf{z}_0 - \mathbf{T}\mathbf{u}_0). \tag{10}$$

where

$$\mathbf{D} = \mathbf{T}^{\mathrm{T}}\mathbf{Q}\mathbf{T} + \mathbf{R} \tag{11}$$

This is a classical version of the HHC algorithm that yields an explicit relation for the optimal control input. Another version of the HHC algorithm where the sensitivity matrix $\mathbf{T}$ is updated using least-squares methods after every control update is known as the adaptive or recursive HHC [10]. In order to describe the adaptive HHC algorithm, relative output and input vectors are defined, $\Delta\mathbf{z}_k$, and $\Delta\mathbf{u}_k$ as

$$\Delta\mathbf{z}_k = \mathbf{z}_k - \mathbf{z}_{k-1}, \;\; \Delta\mathbf{u}_k = \mathbf{u}_k - \mathbf{u}_{k-1}, \tag{12}$$

and, $\Delta\mathbf{Z}_k$ and $\Delta\mathbf{U}_k$ as

$$\begin{aligned} \Delta\mathbf{Z}_k &= \left[\begin{array}{ccc} \Delta\mathbf{z}_1 & \cdots & \Delta\mathbf{z}_k \end{array}\right]^T, \\ \Delta\mathbf{U}_k &= \left[\begin{array}{ccc} \Delta\mathbf{u}_1 & \cdots & \Delta\mathbf{u}_k \end{array}\right]^T. \end{aligned} \tag{13}$$

The relation between the successive updates of vibration levels $\mathbf{z}_k$ is

$$\mathbf{z}_k = \mathbf{z}_{k-1} + \mathbf{T}(\mathbf{u}_k - \mathbf{u}_{k-1}). \tag{14}$$

This can be represented in another form,

$$\Delta \mathbf{z}_k = \mathbf{T}\Delta \mathbf{u}_k. \tag{15}$$

Hence, it follows from Eqs. (15) and (13) that

$$\Delta \mathbf{Z}_k = \mathbf{T}\Delta \mathbf{U}_k. \tag{16}$$

Assuming $\Delta \mathbf{U}_k \Delta \mathbf{U}_k^{\mathrm{T}}$ is nonsingular, one can define

$$\mathbf{P}_k = (\Delta \mathbf{U}_k \Delta \mathbf{U}_k^{\mathrm{T}})^{-1}, \tag{17}$$

and from Eq. (16) the least squares estimate $\hat{\mathbf{T}}_{\mathrm{LS}_k}$ of $\mathbf{T}$ is given by

$$\hat{\mathbf{T}}_{\mathrm{LS}_k} = \Delta \mathbf{Z}_k \Delta \mathbf{U}_k^{\mathrm{T}} \mathbf{P}_k. \tag{18}$$

The recursive least squares method is used to iteratively update $\hat{\mathbf{T}}_{\mathrm{LS}_k}$ based on the past and current values of $\Delta \mathbf{z}_k$ and $\Delta \mathbf{u}_k$. The updated estimate $\hat{\mathbf{T}}_{\mathrm{LS}_k}$ is used at each control update step to calculate the optimal control input $\mathbf{u}_{k,\mathrm{opt}}$ given in Eq. 8. The adaptive HHC algorithm has been shown to perform better than the classical HHC when the model nonlinearities are significant and the sensitivity matrix $\mathbf{T}$ is a poor approximation of the model [10].

Retrospective Cost Adaptive Control

The RCAC algorithm was developed at the University of Michigan over the past 15 years [11–13]. RCAC is a discrete-time adaptive controller that minimizes the performance variable $\mathbf{z}$. The algorithm does not require detailed plant information; instead, RCAC uses knowledge of the Markov parameters of the transfer function G_{zu} which relates the input $\mathbf{u}$ to the performance $\mathbf{z}$.

Consider the MIMO discrete-time system

$$\mathbf{x}(k) = A\mathbf{x}(k-1) + B\mathbf{u}(k-1), \tag{19}$$

$$\mathbf{y}_0(k) = E_1\mathbf{x}(k), \tag{20}$$

$$\mathbf{z}(k) = \mathbf{y}_0(k), \tag{21}$$

where $\mathbf{x}(k) \in \mathbb{R}^{l_x}$ is the state vector, $\mathbf{y}_0(k) \in \mathbb{R}^{l_y}$ is the output vector, $\mathbf{z}(k) \in \mathbb{R}^{l_z}$ is the performance vector, $\mathbf{u}(k) \in \mathbb{R}^{l_u}$ is the input vector, and $k \geq 0$. For $i \geq 1$, define the Markov parameter of G_{zu}

$$\mathcal{H}_i \triangleq E_1 A^{i-1} B. \tag{22}$$

Let n be a positive integer. Then, for all $k \geq n$,

$$\mathbf{x}(k) = A^n \mathbf{x}(k-n) + \sum_{i=1}^{n} A^{i-1} B \mathbf{u}(k-i) \tag{23}$$

thus

$$\mathbf{z}(k) = E_1 A^n \mathbf{x}(k-n) + H\mathbf{U}(k-1), \tag{24}$$

where

$$H \triangleq \begin{bmatrix} \mathcal{H}_1 & \cdots & \mathcal{H}_n \end{bmatrix} \in \mathbb{R}^{l_z \times n l_u}$$

and

$$\mathbf{U}(k-1) \triangleq \begin{bmatrix} \mathbf{u}(k-1) \\ \vdots \\ \mathbf{u}(k-n) \end{bmatrix} \in \mathbb{R}^{n l_u}.$$

Dividing the matrices H and $\mathbf{U}(k-1)$ into known and unknown parts so that

$$H\mathbf{U}(k-1) = H''\mathbf{U}''(k-1) + H'\mathbf{U}'(k-1). \tag{25}$$

where $H' \in \mathbb{R}^{l_z \times l_h l_u}$ and $H'' \in \mathbb{R}^{l_z \times l_u (n-l_h)}$ are the known and unknown Markov parameters respectively and $\mathbf{U}' \in \mathbb{R}^{l_h l_u}$ and $\mathbf{U}'' \in \mathbb{R}^{(n-l_h) l_u}$ are the corresponding control inputs. Next, collecting the unknown parts of the system into

$$\mathcal{S}(k) \triangleq E_1 A^n \mathbf{x}(k-n) + H''\mathbf{U}''(k-1). \tag{26}$$

and rewriting (24) using (25) as

$$\mathbf{z}(k) = \mathcal{S}(k) + H'\mathbf{U}'(k-1). \tag{27}$$

Retrospective Cost

Replacing the controls in $\mathbf{U}'$ in (27) with the retrospective controls $\hat{\mathbf{U}}'$ and defining the *retrospective performance*,

$$\hat{\mathbf{z}}(k) \triangleq \mathcal{S}(k) + H'\hat{\mathbf{U}}'(k-1), \tag{28}$$

Subtracting (27) from (28) and solving for $\hat{\mathbf{z}}(k)$ yields

$$\hat{\mathbf{z}}(k) = \mathbf{z}(k) - H'\mathbf{U}'(k-1) + H'\hat{\mathbf{U}}'(k-1). \tag{29}$$

Then, defining the *retrospective cost function*

$$J_z(\hat{\mathbf{U}}'(k-1), k) \triangleq \hat{\mathbf{z}}^{\mathrm{T}}(k) R(k) \hat{\mathbf{z}}(k), \tag{30}$$

where $R(k) \in \mathbb{R}^{l_z \times l_z}$ is a positive-definite performance weighting. The optimized control values $\hat{\mathbf{U}}'(k-$

1) are then used to compute the next control input $\mathbf{u}(k)$. Given a full column rank H', the global minimizer for the quadratic cost function in (30) is given by

$$\hat{\mathbf{U}}'(k-1) = \left[H'^{\mathrm{T}} R(k) H'\right]^{-1} H'^{\mathrm{T}} R(k) \left[H'\mathbf{U}'(k-1) - \mathbf{z}(k)\right]. \tag{31}$$

Controller Construction

A strictly proper time-series controller of order n_{c} is defined as

$$\mathbf{u}(k) = \theta(k)\phi(k-1), \tag{32}$$

where

$$\theta(k) \triangleq [M_1(k) \cdots M_{n_{\mathrm{c}}}(k)\ N_1(k) \cdots N_{n_{\mathrm{c}}}(k)] \in \mathbb{R}^{l_u \times n_{\mathrm{c}}(l_u+l_z)}, \tag{33}$$

for $M_i(k) \in \mathbb{R}^{l_u \times l_u}$, $N_i(k) \in \mathbb{R}^{l_u \times l_z}$, and

$$\phi(k-1) \triangleq \begin{bmatrix} \mathbf{u}(k-1) \\ \vdots \\ \mathbf{u}(k-n_{\mathrm{c}}) \\ \mathbf{z}(k-1) \\ \vdots \\ \mathbf{z}(k-n_{\mathrm{c}}) \end{bmatrix} \in \mathbb{R}^{n_{\mathrm{c}}(l_u+l_z)}. \tag{34}$$

Next, the *Recursive Least Squares* cumulative cost function is defined as

$$J_{\mathrm{R}}(\theta(k)) \triangleq \left[(\theta(k) - \theta(0))\, P^{-1}(0)\, (\theta(k) - \theta(0))\right]^{\mathrm{T}} + \sum_{i=1}^{k} \|\phi^{\mathrm{T}}(i-2)\theta^{\mathrm{T}}(k) - \hat{\mathbf{u}}^{\mathrm{T}}(i-1)\|^2, \tag{35}$$

where $P(0) \in \mathbb{R}^{n_{\mathrm{c}}(l_u+l_z) \times n_{\mathrm{c}}(l_u+l_z)}$ is the initial covariance matrix. The minimizer for (35) is given by

$$\theta^{\mathrm{T}}(k) \triangleq \theta^{\mathrm{T}}(k-1) + \frac{P(k-1)\phi(k-2)[\theta(k-1)\phi(k-2) - \hat{\mathbf{u}}(k-1)]^{\mathrm{T}}}{[1 + \phi^{\mathrm{T}}(k-2)P(k-1)\phi(k-2)]}. \tag{36}$$

where the error covariance $P(k)$ is updated by

$$P(k) \triangleq P(k-1) - \frac{P(k-1)\phi(k-2)\phi^{\mathrm{T}}(k-2)P(k-1)}{[1 + \phi^{\mathrm{T}}(k-2)P(k-1)\phi(k-2)]}. \tag{37}$$

Controller Implementation

In a typical HHC controller implementation on a 4-bladed rotor the control input vector $\mathbf{u}_k$ consists of 2/rev, 3/rev, 4/rev, and 5/rev harmonic amplitudes of the flap deflection. The output vector $\mathbf{z}_k$ is a combination of the 4/rev vibratory hub shears and moments [5, 9]. However, for simplicity, only the 4/rev harmonic components are used as the input in this study:

$$\mathbf{u}_k = [\delta_{4c}, \delta_{4s}]^T, \tag{38}$$

where δ_{4c} and δ_{4s} are the cosine and sine components of the 4/rev control input harmonic. The total flap deflection is given by

$$\delta(\psi, \mathbf{u}_k) = \delta_{4c}\cos(4\psi) + \delta_{4s}\sin(4\psi). \tag{39}$$

The output vector $\mathbf{z}_k$ consists of cosine and sine components of the 4/rev vertical hub shear:

$$\mathbf{z}_k = \begin{bmatrix} F_{HZ4c} \\ F_{HZ4s} \end{bmatrix}. \tag{40}$$

Since the HHC controller is based on a linear quasi-steady approximation of the helicopter rotor model, it is essential to let the rotor reach a steady state after every control update. In the AVINOR code, the sampling time between two consecutive control updates is typically chosen to be 6-8 revolutions. A continuous-time HHC (CTHHC) controller which updates the control inputs at every time-step, instead of waiting for a few revolutions, was developed by Hall and Wereley in [17]. The CTHHC was compared and found to yield similar vibration reduction performance as the conventional discrete-time HHC. Since the output vector consists of the 4/rev harmonic components of the vertical hub shear (Eq. 40), using a CTHHC controller requires implementing "real-time" Fourier analysis in the AVINOR code and has been avoided in this study.

The RCAC controller has been tested on several linear time-invariant (LTI) systems [12, 13]. It is an adaptive controller and needs little information (first few Markov parameters) about the system. In

this study, a linear approximation of the helicopter rotor model at a given flight condition, represented by the **T** matrix in Eq. 1, is provided to the controller. Using the fact that the RCAC controller is adaptive, the sampling time between two consecutive RCAC control updates is set to 1 revolution. The RCAC controller can also potentially be used as a continuous time-domain controller that updates the absolute flap deflection at every time-step, instead of its harmonic components. However, similar to the CTHHC, it will require implementation of "real-time" Fourier analysis in the AVINOR code in order to calculate the 4/rev vibratory loads at every time-step. Also, working with a more complicated model of the rotor which includes all the hub shears and moments as the output variables and the 2/rev-5/rev harmonic components of the flap deflection as the input variables would require further retuning of the RCAC parameters and therefore will be pursued in a future research study.

Results and Discussions

The results presented in this section are obtained for a helicopter configuration resembling a full-scale four-bladed MBB BO-105 hingeless rotor. The rotor parameters are listed in Table 1. All the values in the table (except C_W, γ, and σ) have been nondimensionalized using M_b, L_b, and $1/\Omega$ for mass, length and time, respectively. The mass and stiffness distributions are assumed to be constant along the span of the blade. The rotor is trimmed using a propulsive trim procedure. The vibratory hub shears and moments are obtained from the integration of the distributed inertial and aerodynamic loads over the entire blade span in the rotating frame. Subsequently, the loads are transformed to the hub-fixed non-rotating system, and the contributions from the individual blades are combined. In this process, the blades are assumed to be identical. Active vibration reduction studies are performed using a single 20%c conventional plain trailing-edge flap, shown in Fig. 2 and its spanwise configuration is shown in Fig. 3.

Time histories of the 4/rev vertical hub shear sine and cosine components calculated when using the RCAC and HHC controllers are shown in Figs. 4(a) and 4(b), respectively for a descending flight at $\mu = 0.15$ and descent angle 6.5°. Both the controllers reduce the vertical hub shear components by up to 99%. The RCAC controller exhibits more transients

Table 1: Rotor parameters used for noise and vibration reduction studies.

Dimensional Rotor Data	
$R = 4.91$ m	
$M_b = 27.35$ kg	
$\Omega = 425$ RPM	
Nondimensional Rotor Data	
$N_b = 4$	$L_b = 1.0$
$c_b/R = 0.05498$	$\theta_{\text{tw}} = -8°$
$e = 0$	
$X_A = 0$	$X_{Ib} = 0$
$\omega_F = 1.124, 3.40, 7.60$	$\omega_L = 0.732, 4.458$
$\omega_T = 3.17, 9.08$	
$\gamma = 5.5$	$\sigma = 0.07$
$\beta_p = 2.5°$	
Helicopter Data	
$C_W = 0.005$	$fC_{df} = 0.031$
$X_{FA} = 0.0$	$Z_{FA} = 0.3$
$X_{FC} = 0.0$	$Z_{FC} = 0.3$

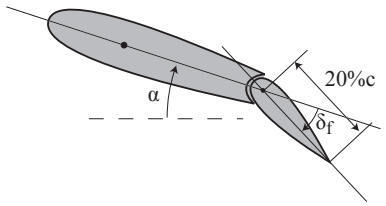

Figure 2: A 20%c conventional plain flap configuration.

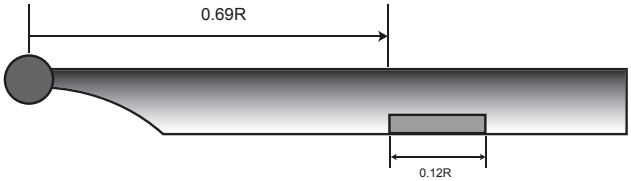

Figure 3: Single spanwise configuration of the 20%c plain flap on the rotor blade.

compared to the HHC controller but is faster to converge. Convergence time for the RCAC controller can be reduced by scaling the $\mathbf{T}$ matrix. For this particular simulation, the $\mathbf{T}$ matrix was scaled by a factor of 0.1. The RCAC controller used is of order 5 and the parameters $\eta = 1.0$ and $P_1 = 5.0$.

The corresponding 4/rev flap deflection component time histories are shown in Figs. 5(a) and 5(b). It is interesting to note that the converged values of the harmonic flap deflection components are very similar for both the controllers. Flap deflection histories over one complete rotor revolution obtained at the end of simulations using the relation $\delta(\psi) = \delta_{4c}\cos(4\psi) + \delta_{4s}\sin(4\psi)$ are shown in Fig. 6. Note that the controllers yield very similar flap deflection histories with the peaks and valleys appearing at the same azimuth locations. The flap deflection is restricted to lie within $\pm 4^\circ$. Finally, the effect of reducing the vertical hub shear on the other hub shears and moments is examined. The non-dimensional 4/rev vibratory hub shears and moments obtained during active control using the two control approaches are compared in Fig. 7. The controllers show similar effects on all the hub shears and moments.

Similar comparisons are performed for a high-speed level cruise flight at $\mu = 0.30$. Time histories of the 4/rev vertical hub shear sine and cosine components calculated when using the RCAC and HHC controllers are shown in Figs. 8(a) and 8(b), respectively. Both the controllers reduce the vertical hub shear components by up to 99%. The RCAC controller used is of order 5 and the parameters $\eta = 10.0$ and $P_1 = 4.0$. The corresponding 4/rev flap deflection component time histories are shown in Figs. 9(a) and 9(b). Like in the case of the descending flight condition, the converged values of the flap deflection components are very similar for both the controllers. Flap deflection histories over a complete rotor revolution obtained at the end of simulations are shown in Fig. 10. Note that the controllers yield very similar flap deflection histories with the peaks and valleys appearing at the same azimuth locations. Finally, the effect of reducing the vertical hub shear on the other hub shears and moments is examined. The non-dimensional 4/rev vibratory hub shears and moments obtained during active control using the two control approaches are compared in Fig. 11. The controllers show similar effects on all the hub shears and moments.

Robustness of the RCAC and HHC controllers to errors in the $\mathbf{T}$ matrix is compared at a low-speed descending flight condition with $\mu = 0.15$, descent angle 6.5°, and weight coefficient $C_W = 0.005$. The $\mathbf{T}$ matrix for this flight condition is

$$\mathbf{T} = \begin{bmatrix} -0.0134 & 0.0397 \\ -0.044 & -0.0043 \end{bmatrix}. \tag{41}$$

An error is added to the various terms in the matrix as shown below

$$\mathbf{T} = \begin{bmatrix} T_{11}(1+\alpha_{11}) & T_{12}(1+\alpha_{12}) \\ T_{21}(1+\alpha_{21}) & T_{22}(1+\alpha_{22}) \end{bmatrix}, \tag{42}$$

and the robustness of the controllers to these errors is examined. The performance of the controllers for α_{11} ranging from -21 to 21 is compared in Fig. 12. This range of values was obtained using a trial and error approach until one of the controllers fails to reduce any vibrations. Both the controllers show significant vibration reduction for $|\alpha_{11}| \leq 14$. However, only the RCAC controller is capable of vibration reduction for $\alpha_{11} = 21$. Overall the RCAC controller exhibits better performance when compared to the HHC controller. The RCAC controller used is of the order 5 with parameters $\eta = 2.2$ and $P_1 = 0.5$. Note that the RCAC controller takes longer to converge compared to the HHC controller. As mentioned earlier, convergence times for the RCAC controller can be reduced by scaling the $\mathbf{T}$ matrix. However, scaling was not attempted in these robustness tests in order to avoid scaling the errors in the $\mathbf{T}$ matrix. Performance of the controllers for α_{22} ranging from -21 to 21 is compared in Fig. 13. Both the controllers yield significant vibration reduction for positive error values. The RCAC controller shows better performance compared to the HHC controller for negative values of α_{22}. The RCAC controller used is of the order 5 with parameters $\eta = 2.0$ and $P_1 = 0.5$.

The performance of the controllers for α_{21} ranging from -6 to 6 is compared in Fig. 14. Both the controllers show significant vibration reduction for positive values of α_{21} and neither controller shows any vibration reduction for negative error values. This demonstrates that the controllers are able to reduce the vibrations as long as there is no change in the sign of the term T_{21}. Hence, it is important to know the sign of the off-diagonal $\mathbf{T}$ matrix elements accurately. The RCAC controller used is of the order 8 with parameters $\eta = 2.0$ and $P_1 = 1.0$. The performance of the controllers for α_{12} ranging from -6 to 6 is compared in Fig. 15. Both the controllers show significant vibration reduction for positive values of α_{12} and neither controller shows any vibration

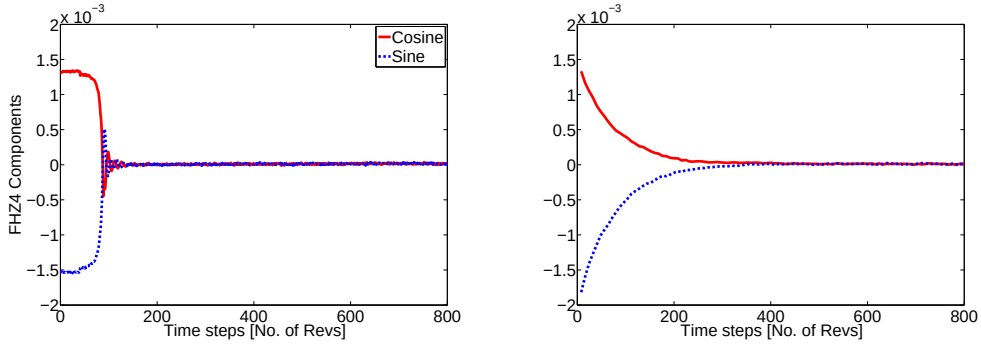

(a) RCAC (b) HHC

Figure 4: Time histories of the 4/rev vertical hub shear components obtained using the HHC and RCAC controllers during a descending flight at an advance ratio $\mu = 0.15$ and descent angle 6.5°.

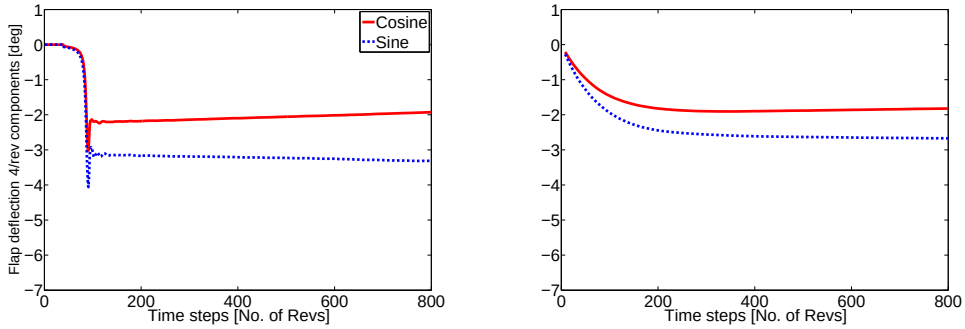

(a) RCAC (b) HHC

Figure 5: Time histories of the 4/rev flap deflection component amplitudes obtained using the HHC and RCAC controllers during a descending flight at an advance ratio $\mu = 0.15$ and descent angle 6.5°.

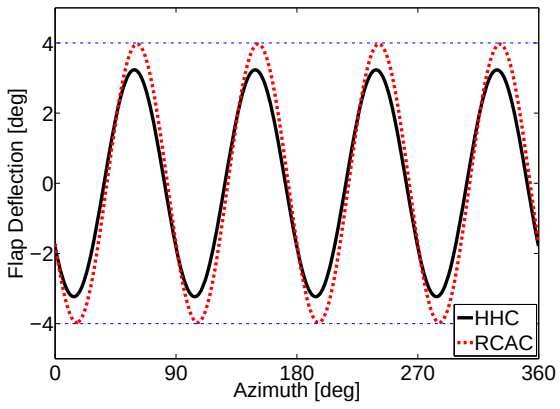

Figure 6: Flap deflection histories over a rotor revolution obtained from the HHC and RCAC control approaches at a heavy BVI descending flight condition with $\mu = 0.15$ and descent angle 6.5°.

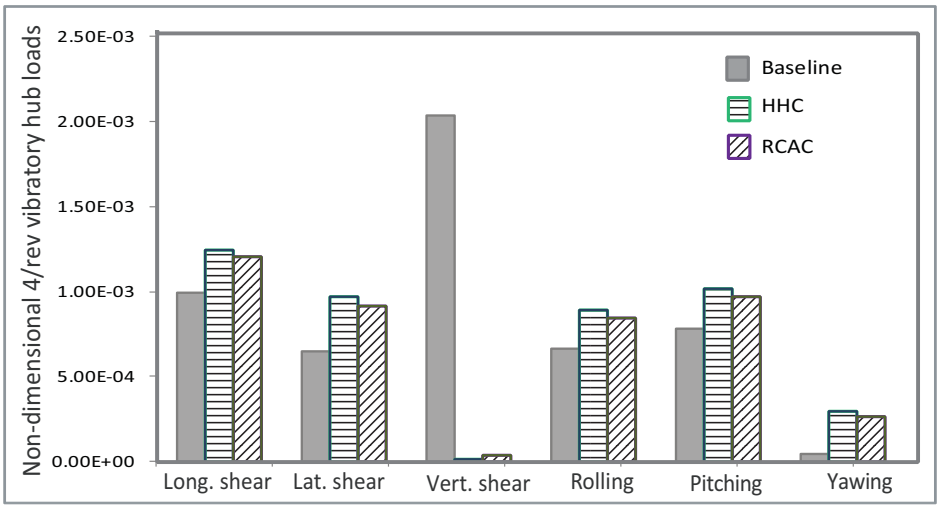

Figure 7: Reduction in 4/rev vertical hub shear obtained using the HHC and RCAC controllers with a single plain flap in descending flight at $\mu = 0.15$ and descent angle 6.5°.

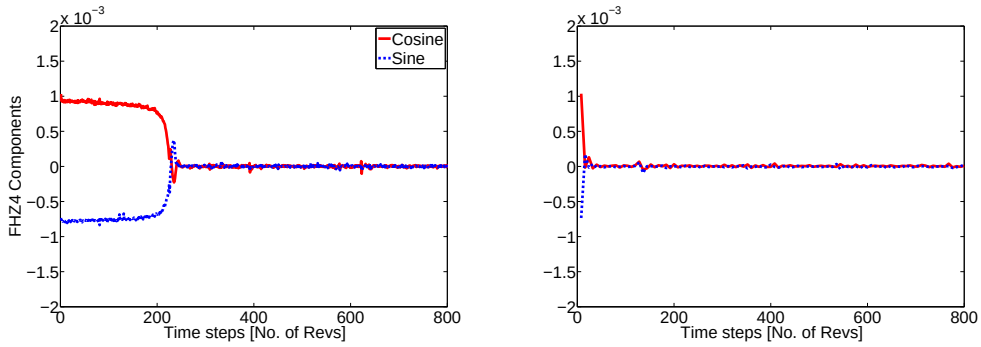

(a) RCAC (b) HHC

Figure 8: Time histories of the 4/rev vertical hub shear components obtained using the HHC and RCAC controllers during a high-speed cruise flight at $\mu = 0.30$.

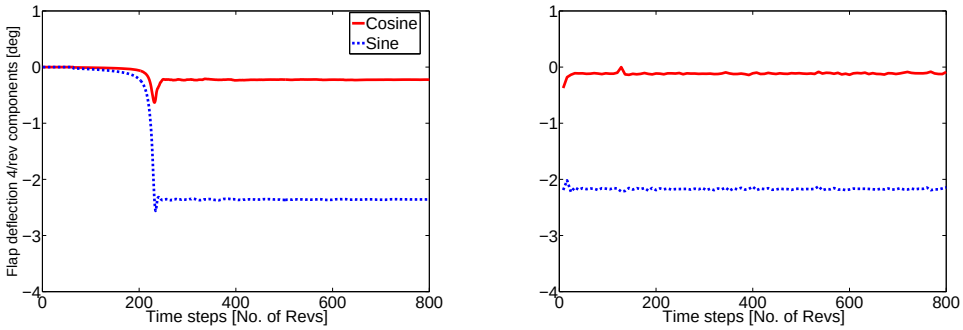

(a) RCAC (b) HHC

Figure 9: Time histories of the 4/rev flap deflection component amplitudes obtained using the HHC and RCAC controllers during a high-speed cruise flight at $\mu = 0.30$.

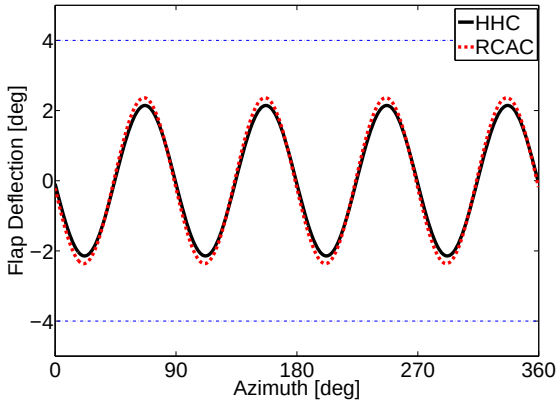

Figure 10: Flap deflection histories over a rotor revolution obtained from the HHC and RCAC control approaches at a high-speed cruise flight condition at $\mu = 0.30$.

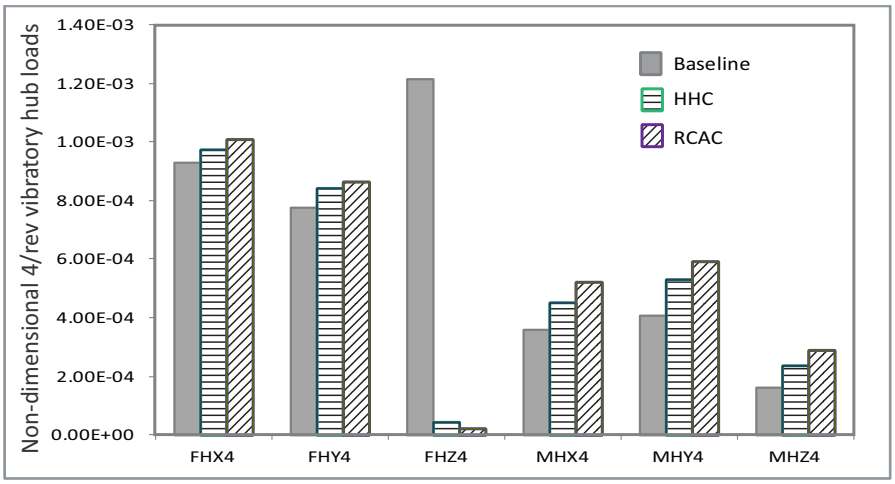

Figure 11: Reduction in 4/rev vertical hub shear obtained using the HHC and RCAC controllers with a single plain flap in a high-speed cruise flight at $\mu = 0.30$.

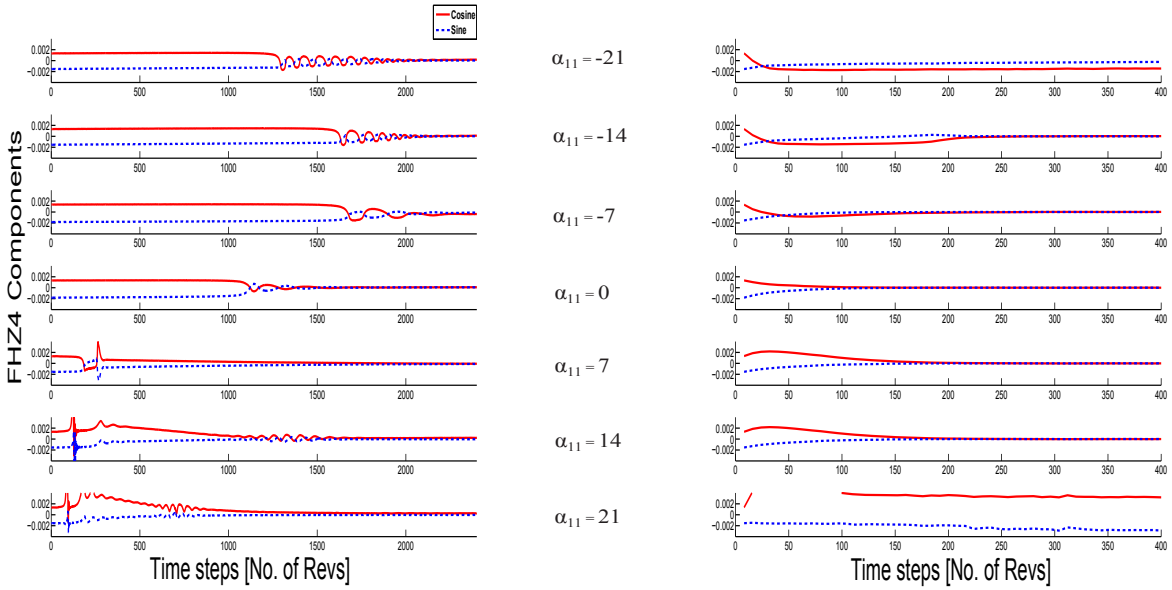

(a) RCAC (b) HHC

Figure 12: Reduction in 4/rev vertical hub shear components using the HHC and RCAC controllers for variation in the error term $\alpha_{\mathbf{11}}$ at a descending flight with $\mu = 0.15$ and $C_W = 0.005$.

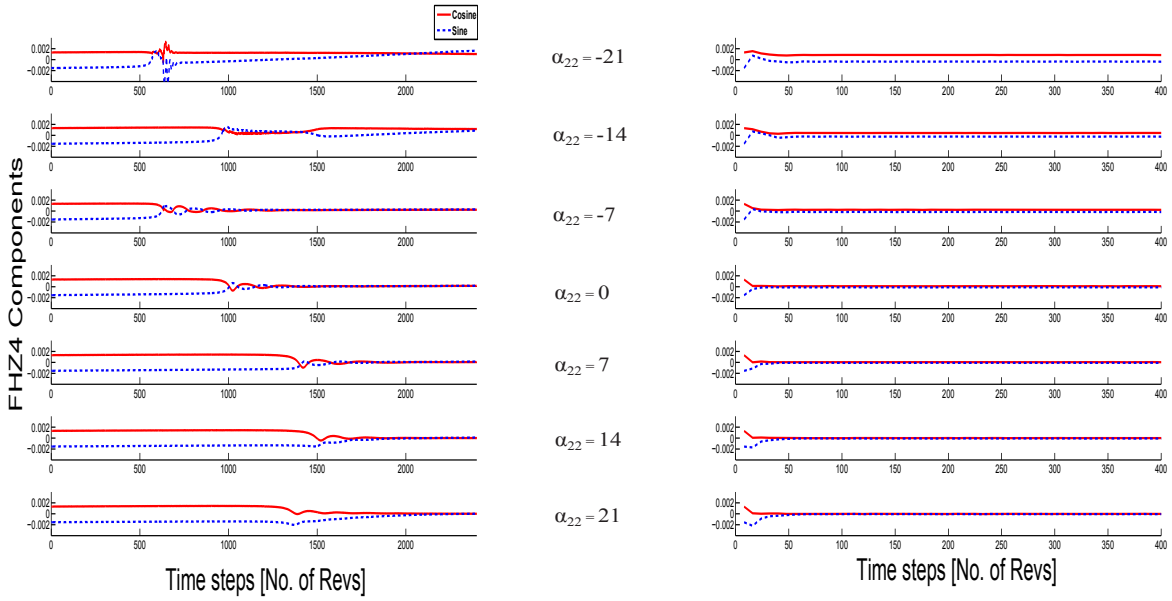

(a) RCAC (b) HHC

Figure 13: Reduction in 4/rev vertical hub shear components using the HHC and RCAC controllers for variation in the error term $\alpha_{\mathbf{22}}$ at a descending flight with $\mu = 0.15$ and $C_W = 0.005$.

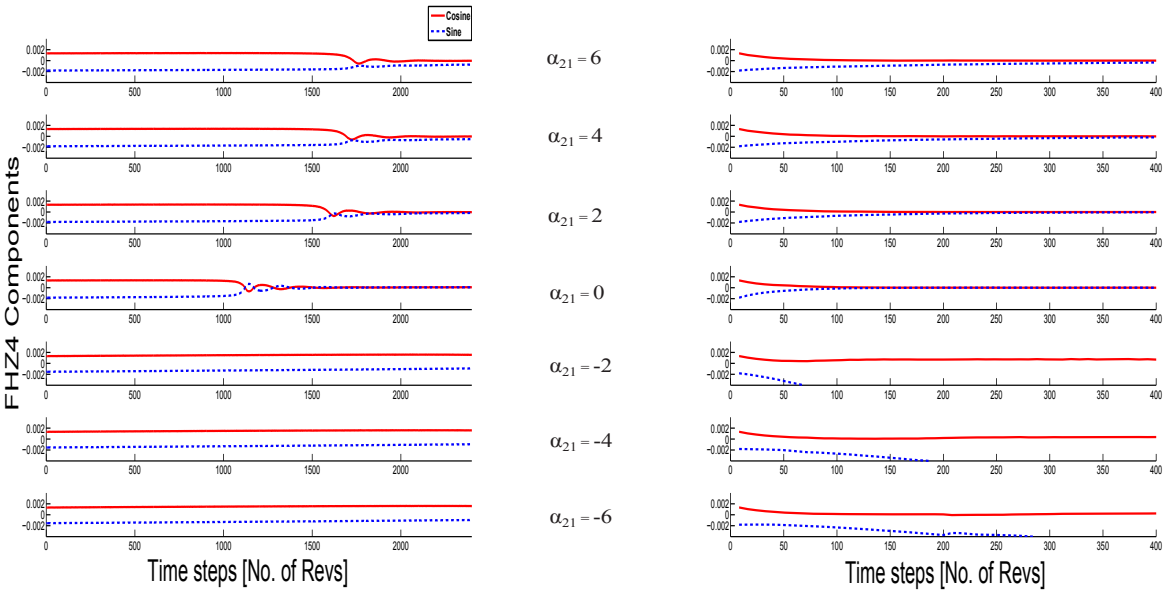

(a) RCAC (b) HHC

Figure 14: Reduction in 4/rev vertical hub shear components using the HHC and RCAC controllers for variation in the error term $\alpha_{\mathbf{21}}$ at a descending flight with $\mu = 0.15$ and $C_W = 0.005$.

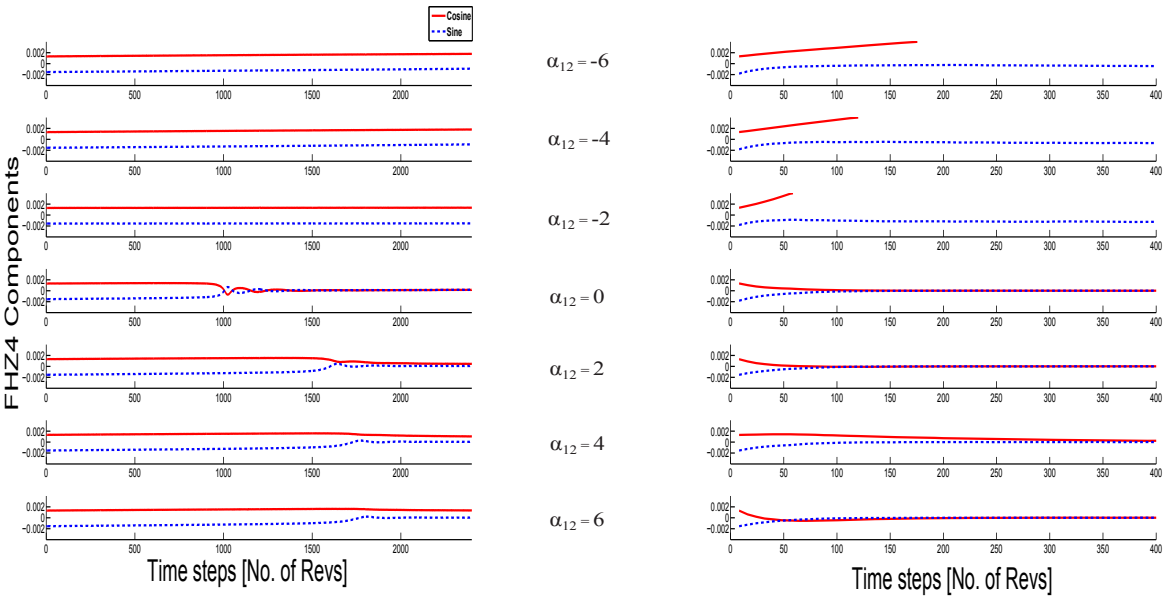

(a) RCAC (b) HHC

Figure 15: Reduction in 4/rev vertical hub shear components using the HHC and RCAC controllers for variation in the error term $\alpha_{\mathbf{12}}$ at a descending flight with $\mu = 0.15$ and $C_W = 0.005$.

reduction for negative error values. This is consistent with the observation made earlier that the controllers fail to perform if the errors cause a change in the sign of the $\mathbf{T}$ matrix elements. The RCAC controller used is of the order 8 with parameters $\eta = 2.0$ and $P_1 = 1.4$. It is interesting to note from the above simulation results that the controllers are more tolerant of errors in the diagonal terms than those in the off-diagonal terms. For instance the RCAC controller is able to reduce the vibrations for $\alpha_{11} = 21$ or $\alpha_{22} = 21$ but fails to do so for $\alpha_{21} = 2$ or $\alpha_{12} = -2$. That is, the controller performance is insensitive to the value of the diagonal terms which implies that only the 4/rev cosine component of the flap deflection can effectively reduce the 4/rev sine component of the vertical hub load and only the 4/rev sine component of the flap deflection can effectively reduce the 4/rev cosine component of the vertical hub load.

Next, the robustness of the RCAC and HHC controllers to a variation in the weight coefficient (C_W) is compared at a low-speed descending flight condition with $\mu = 0.15$ and descent angle 6.5°. The $\mathbf{T}$ matrix is evaluated for a weight coefficient $C_W = 0.005$, and the vibration reduction performance of the two controllers is compared for $0.0035 \leq C_W \leq 0.0065$, as shown in Fig. 16. Both the controllers perform well for $C_W \leq 0.006$ reducing the 4/rev vertical hub shear by upto 95%. At $C_W = 0.0065$, the RCAC controller does not yield any significant reduction whereas the HHC controller yields up to 80% reduction.

Conclusions

A Retrospective Cost Adaptive Control (RCAC) algorithm is tested for helicopter vibration reduction applications. The RCAC is compared to the widely used higher harmonic control (HHC) algorithm in terms of vibration reduction capabilities at both low-speed and high-speed flight conditions. Robustness of the two controllers to modeling errors is compared. The principal conclusions of the study are summarized below:

1. The RCAC controller reduces the 4/rev vertical hub shear components by up to 99% at a low-speed descending flight condition with $\mu = 0.15$ as well as at a high-speed level flight condition with $\mu = 0.30$.

2. The RCAC and HHC controllers yield similar vibration reduction levels. The controllers yield similar steady state flap deflections with less than 10% difference in the amplitude. The controllers also show similar effects on all the hub shears and moments.

3. The RCAC shows better vibration reduction performance in the presence of modeling errors introduced through the $\mathbf{T}$ matrix. Both the controllers are equally robust to errors in the off-diagonal terms, however, the RCAC shows better tolerance to errors in the diagonal terms.

4. In the case of off-diagonal terms, the controllers perform well as long as the modeling errors do not cause a sign change. Hence, it is important to identify the sign of the off-diagonal terms accurately.

5. The controllers are more tolerant of errors in the diagonal terms than of those in the off-diagonal terms. For instance, the RCAC controller is able to reduce the vibrations for $\alpha_{11} = 21$ or $\alpha_{22} = 21$ but fails to do so for $\alpha_{21} = 2$ or $\alpha_{12} = -2$. Thus, the diagonal terms are not critical to the controller's performance which means that only the 4/rev cosine component of the flap deflection can be used to reduce the 4/rev sine component of the vertical hub load whereas only the 4/rev sine component of the flap deflection can be used to reduce the 4/rev cosine component of the vertical hub load.

6. The HHC shows slightly better robustness to a variation in the weight coefficient compared to RCAC.

These conclusions demonstrate that the RCAC is as effective as the HHC in reducing helicopter vibrations and shows better robustness to certain modeling errors. Thus, it is a viable alternative to the HHC and can potentially perform better in missions involving significant variations in the rotor vibration characteristics. Future work on the potential of this interesting approach is warranted particularly for non-steady state flight conditions.

Acknowledgments

This research was supported by the Vertical Lift Research Center of Excellence (VLRCOE) sponsored

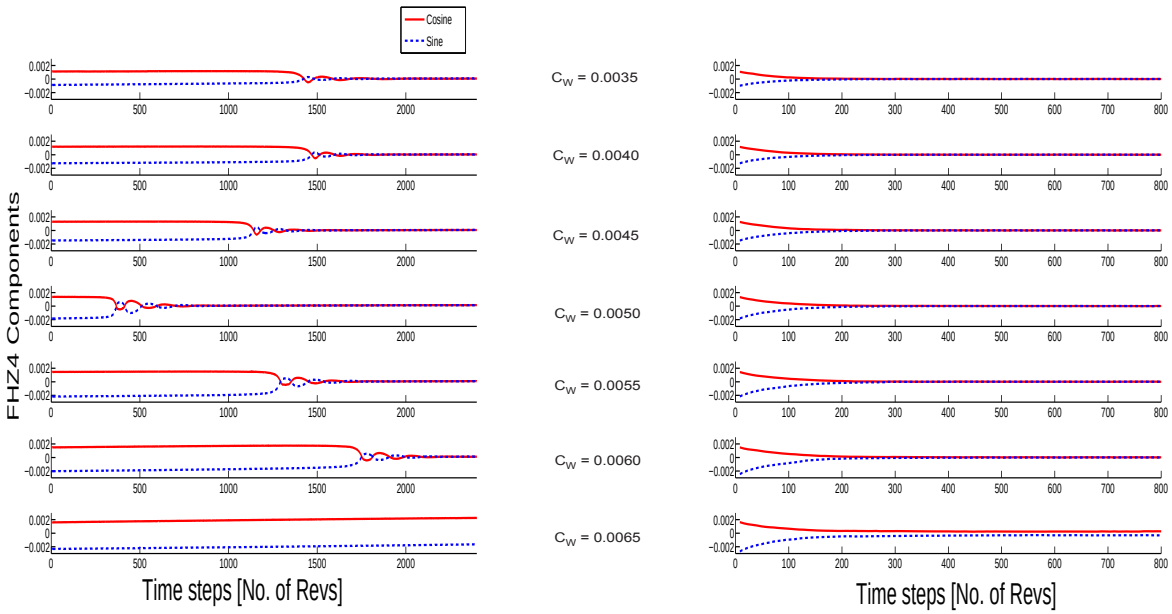

(a) RCAC

(b) HHC

Figure 16: Reduction in 4/rev vertical hub shear components using the HHC and RCAC controllers for variations in the weight coefficient (C_W) where the $\mathbf{T}$ matrix is calculated at $C_W = 0.005$, descending flight at $\mu = 0.15$.

by NRTC and U.S. Army with Dr. John Berry as grant monitor.

REFERENCES

1. Friedmann, P. P. and Millott, T. A. , "Vibration Reduction in Rotorcraft Using Active Control: A Comparison of Various Approaches," Journal of Guidance, Control, and Dynamics, Vol. 18, (4), July-August 1995, pp. 664–673.

2. Splettstoesser, W. , Kube, R. , Wagner, W. , Seelhorst, U. , Boutier, A. , Micheli, F. , Mercker, E. , and Pengel, K. , "Key Results From a Higher Harmonic Control Aeroacoustic Rotor Test (HART)," Journal of the American Helicopter Society, Vol. 42, (1), January 1997, pp. 58–78.

3. Swanson, S. M. , Jacklin, S. A. , Blaas, . , Niesl, G. , and Kube, R. , "Reduction of Helicopter BVI Noise, Vibration, and Power Consumption through Individual Blade Control," Proceedings of the 51st Annual Forum of the American Helicopter Society, Fort Worth, TX, May 1995, pp. 662–680.

4. Jacklin, S. A. , Haber, A. , de Simone, G. , Norman, T. , Kitaplioglu, C. , and Shinoda, P. , "Full-Scale Wind Tunnel Test of an Individual Blade Control System for a UH-60 Helicopter," Proceedings of the 51st Annual Forum of the American Helicopter Society, Montreal, Canada, June 2002.

5. Patt, D. , Liu, L. , and Friedmann, P. P. , "Simultaneous Vibration and Noise Reduction in Rotorcraft Using Aeroelastic Simulation," Journal of the American Helicopter Society, Vol. 51, (2), April 2006, pp. 127–140.

6. Koratkar, N. A. and Chopra, I. , "Wind Tunnel Testing of a Smart Rotor Model with Trailing Edge Flaps," Journal of the American Helicopter Society, Vol. 47, (4), October 2002, pp. 263–272.

7. Straub, F. K. , Anand, V. , Birchette, T. S. , and Lau, B. H. , "Wind Tunnel Test of the SMART Active Flap Rotor," Proceedings of the 65th American Helicopter Society Annual Forum, Grapevine,TX, May 2009.

8. Shin, S. J. , Cesnik, C. E. S. , and Hall, S. R. , "Closed-Loop Control Tests of the

NASA/ARMY/MIT Active Twist Rotor for Vibration Reduction," Proceedings of the American Helicopter Society 59th Annual Forum, Phoenix, AZ, June 2003.

9. Padthe, A. K. , Liu, L. , and Friedmann, P. P. , "Numerical Evaluation of Microflaps for On Blade Control of Noise and Vibration," Proceedings of the 52nd AIAA/ASME/ASCE/AHS/ACS Structures, Structural Dynamics and Materials Conference, Denver, CO, April 2011.

10. Patt, D. , Liu, L. , Chandrasekar, J. , Bernstein, D. S. , and Friedmann, P. P. , "Higher-Harmonic-Control Algorithm for Helicopter Vibration Reduction Revisited," Journal of Guidance, Control, and Dynamics, Vol. 28, (5), September-October 2005, pp. 918–930.

11. Hoagg, J. B. and Bernstein, D. S. , "Retrospective Cost Model Reference Adaptive Control for Nonminimum-Phase Systems," Journal of Guidance, Control, and Dynamics, Vol. 35, (6), Nov-Dec 2012, pp. 1767–1786.

12. Santillo, M. A. and Bernstein, D. S. , "Adaptive Control Based on Retrospective Cost Optimization," Journal of Guidance, Control, and Dynamics, Vol. 33, (2), Mar-Apr 2010, pp. 289–304.

13. D'Amato, A. M. , Sumer, E. D. , and Bernstein, D. S. , "Frequency-Domain Stability Analysis of Retrospective-Cost Adaptive Control for Systems with Unknown Non-Minimum Phase Zeros," Proceedings of the 50th IEEE Conference on Decision and Control, Orlando, FL, Dec 2011, pp. 1098–1103.

14. Glaz, B. , Friedmann, P. P. , Liu, L. , Kumar, D. , and Cesnik, C. E. S. , "The AVINOR Aeroelastic Simulation Code and Its Application to Reduced Vibration Composite Rotor Blade Design," Proceedings of the 50th AIAA/ASME/ASCE/AHS/ACS Structures, Structural Dynamics and Materials Conference, Palm Springs, CA, May 2009. AIAA Paper No. 2009-2601.

15. de Terlizzi, M. and Friedmann, P. P. , "Active Control of BVI Induced Vibrations Using a Refined Aerodynamic Model and Experimental Correlation," American Helicopter Society 55th Annual Forum Proceedings, Montreal, Canada, May 25-27 1999, pp. 599–615.

16. Myrtle, T. F. and Friedmann, P. P. , "Application of a New Compressible Time Domain Aerodynamic Model to Vibration Reduction in Helicopters Using an Actively Controlled Flap," Journal of the American Helicopter Society, Vol. 46, (1), January 2001, pp. 32–43.

17. Hall, S. R. and Wereley, N. M. , "Linear Control Issues in the Higher Harmonic Control of Helicopter Vibrations," Proceedings of the 45th Annual Forum of the American Helicopter Society, Boston, MA, May 1989.